

Supplementary Information

A photo-activated nanohybrid for dual-nuclei MR/US/PA multimodal-guided photothermal therapy

Shizhen Chen^{a,b,c+}, Maosong Qiu^{a,b+}, Ruifang Wang^{a,b}, Lei Zhang^{a,b,c}, Conggang Li^{a,b,c},
Chaohui Ye^{a,b,c}, Xin Zhou^{a,b,c*}

^a Key Laboratory of Magnetic Resonance in Biological Systems, State Key Laboratory of Magnetic Resonance and Atomic and Molecular Physics, National Center for Magnetic Resonance in Wuhan, Wuhan Institute of Physics and Mathematics, Innovation Academy for Precision Measurement Science and Technology, Chinese Academy of Sciences-Wuhan National Laboratory for Optoelectronics, Wuhan 430071, P. R. China.

^b University of Chinese Academy of Sciences, Beijing 100049, P. R. China.

^c Optics Valley Laboratory, Hubei 430074, P.R. China.

* Corresponding author

⁺ These authors contributed equally to this work

Table of Contents

Chemicals and reagents	S-3
Fabrication of PFC@PPy@BSA	S-3
Characterization of PFC@PPy@BSA	S-3
SDS-PAGE and coomassie bright blue staining	S-4
Measurement of the photothermal performance of PFP@PPy@BSA	S-4
Fluoride quantification of PFC@PPy@BSA	S-5
¹⁹ F NMR relaxation time	S-6
<i>In vitro</i> NIR laser-induced bubble generation	S-6
Cell culture, cytotoxicity assessment, and cellular uptake study	S-6
<i>In vitro</i> photothermal therapeutic efficiency	S-8
Animal and tumor model	S-9
Characterization of orthotopic NSCLC model mice	S-9
Hemolysis assay	S-10
Statistical analysis	S-11

Chemicals and reagents

All chemicals were used without any further purification unless otherwise stated. Perfluoropentane (PFP), perfluorononane (PFN), and perfluoro-15-crown-5 (PFCE) were purchased from Tokyo Chemical industry Co., Ltd. Perfluorohexane (PFH) was obtained from Macklin (Shanghai, China). Perfluorooctane bromide (PFOB), polyvinyl alcohol (PVA), $\text{FeCl}_3 \cdot 6\text{H}_2\text{O}$, pyrrole monomer, and bovine serum albumin (BSA) were ordered from Sigma-Aldrich (MO, USA). Deionized water (Millipore) was employed in all experiments with a resistivity of $18.2 \text{ M}\Omega \cdot \text{cm}$.

Fabrication of PFC@PPy@BSA

Firstly, 200 μL PFCs were added into 5 mL 5 wt. % PVA aqueous solution, respectively. The PFC emulsion was generated by pulsed sonication 2 s on, 2 s off, for a total of 40 min. The synthesized emulsion was then added to 15 mL water under 4 $^\circ\text{C}$, followed by 1 mL 0.8 M FeCl_3 . After stirring for 30 min, add 28 μL pyrrole monomer and continue stirring at 4 $^\circ\text{C}$ for 24 h. After that, 200 mg of bovine serum albumin was added to the solution. After stirring for 12 h, the resulting suspension was centrifuged at 2000 rpm for 10 min, and the precipitate was washed three times with deionized water. The obtained PFC@PPy@BSA nanoparticles were redispersed in deionized water or PBS buffer (pH = 7.4) for further use.

Characterization of PFC@PPy@BSA

Transmission electron microscopy (TEM) images were obtained on a Tecnai G² 20 TWIN microscope (FEI Company, USA). Ultraviolet-visible-near infrared

(UV–vis–NIR) absorption spectra were performed on an Evolution 220 UV–vis spectrophotometer (Thermo Fisher Scientific Inc., USA). Zeta potential and dynamic light scattering (DLS) measurements were acquired on a ZS nanohybrid analyzer (Malvern, England). ^{19}F NMR and relaxation time were measured on a Bruker Ascend WB 500 MHz spectrometer. All *in vitro* and *in vivo* ^{19}F MRI, ^{129}Xe NMR, and ^{129}Xe Hyper-CEST MRI experiments were performed on a 9.4 T micro-imaging system (Bruker Avance 400, Ettlingen, Germany).

SDS-PAGE and coomassie bright blue staining

The protein expression profiles of PFP@PPy@BSA and BSA were analyzed by SDS-PAGE and Coomassie bright blue staining. Briefly, the PFP@PPy@BSA and BSA samples plus the SDS-PAGE gel loading buffer were heated in a boiling water bath for 20 min. The 12% polyacrylamide gel was used to separate the proteins by the Mini-PROTEAN Tetra System (BIO-RAD, CA, USA). After that, the protein gel was stained with the Coomassie brilliant blue and imaged.

Measurement of the photothermal performance of PFP@PPy@BSA

The PFP@PPy@BSA PBS solutions at different concentrations (1 mL) were exposed to an 808 nm NIR laser at 1 W/cm² for 3 min, respectively. Another experiment was performed using a 250 µg/mL PFP@PPy@BSA PBS solution (1 mL) that was irradiated by different power densities of NIR laser. Besides, 250 µg/mL of PFP@PPy@BSA PBS solution (1 mL) was illuminated by NIR laser at 1 W/cm² for six cycles to examine its photothermal stability. A laser energy meter (Coherent Inc.,

CA, USA) was employed to determine the NIR laser power density. The real-time temperatures of the solutions were recorded using an infrared thermal imaging system.

Photothermal conversion efficiency (η) of PFP@PPy@BSA nanohybrid was evaluated according to a previous method in the literature. Briefly, 125 $\mu\text{g/mL}$ of PFP@PPy@BSA PBS solution (1 mL) was irradiated (808 nm, 1 W/cm^2) for 10 min until the temperature reached a steady state. Afterward, the laser was turned off, and the solution was allowed to cool down for 20 min naturally. Then η was calculated using the equation:

$$\eta = \frac{hA(T_{\max} - T_s) - Q_0}{I(1 - 10^{-A_{808}})}$$

Where h and A represent the heat transfer coefficient and surface area of the container, respectively. T_s and T_{\max} are the solution's initial and maximum steady-state temperatures. Q_0 represents the heat dissipated from light absorbed by the solvent and the cuvette cell, while I and A_{808} represent the power density of the laser and absorbance of the sample at 808 nm, respectively.

Fluoride quantification of PFC@PPy@BSA

To determine the exact concentration of PFC in PFC@PPy@BSA, the ^{19}F NMR was used to test the sample using 2,2,2-trifluoroethanol (at -76.7 ppm) as an internal standard (Figure S4). The absolute encapsulation efficiency of PFCs was calculated using Eq [1]:

$$\eta_{\text{PFC}} = \frac{n}{n_0} \quad \text{Eq [1]}$$

(n_0 is the theoretically content of PFC)

All the ^{19}F NMR experiments were performed on a Bruker Ascend WB 500 MHz spectrometer.

^{19}F NMR relaxation time

A total of 400 μL of PFC@PPy@BSA aqueous solution ($C_{\text{PFP}} = 5 \text{ mM}$) was placed in a 5 mm NMR sample tube (J&K Scientific), and 100 μL D_2O was added to the magnetic field locking control unit. After mixing evenly, T_1 and T_2 of PFC@PPy@BSA (PFC: $-\text{CF}_3$ or $-\text{CF}_2$) were measured by the inversion recovery method and spin-echo method on a 500 MHz spectrometer at different temperatures, respectively (Figure S5).

***In vitro* NIR laser-induced bubble generation**

The PFP@PPy@BSA aqueous solution was dropped onto a glass slide and covered with a coverslip. After irradiating an 808 nm NIR laser at $1 \text{ W}/\text{cm}^2$ for 5 min, the exposure region was captured with an optical microscope (Figure S8).

Cell culture, cytotoxicity assessment, and cellular uptake study

The A549 cells and MRC-5 cells were purchased from the cell bank of the Chinese academy of sciences (Shanghai, China) and cultured in MEM or DMEM medium, supplemented with 10% inactivated fetal bovine serum, 100 U/mL penicillin, and 100 U/mL streptomycin under a humidified air with 5% CO_2 at 37 °C. All agents were

purchased from Boster Company (China) and filtered with a 0.2 μm sterile filter before incubation with cells. The cytotoxicity of PFP@PPy@BSA on A549 cells and MRC-5 cells was determined by the standard MTT and CCK8 assay, respectively (Figure S10). The A549 and MRC-5 cells were seeded in 96-well culture plates at a density of approximately 1×10^4 cells per well and incubated for 24 h.

The PFP@PPy@BSA stock solution was diluted to 1.1, 2.2, 4.5, 9.0, and 18.0 mM based on PFP concentration using either DMEM or MEM and added to the 96- plate wells. Cells cultured with MEM or DMEM media were used as control. As for the MTT method, 200 μL of the culture medium containing 0.5 mg/mL MTT was added to the wells, and the cells were incubated for 4 h at 37 $^{\circ}\text{C}$. Then the media was carefully removed, and 200 μL of DMSO was added to each well. After completely dissolving formazan crystals, each well's optical density at 490 nm was recorded on the ELISA plate reader (Spectra MAX 190, Molecular Devices).

As for the CCK8 assay, 200 μL of the culture medium containing 20 μL CCK8 was added to the wells, and cells were incubated for 2 h at 37 $^{\circ}\text{C}$. Finally, each well's optical density at 450 nm was recorded on the ELISA plate reader (Spectra MAX 190, Molecular Devices). For both MTT and CCK8 assays, the cell viabilities of test groups were assessed as the percentages of viable cells. All data are presented as mean \pm SEM, $n > 3$.

For the cellular uptake of PFP@PPy@BSA, A549 cells or MRC-5 cells were treated with PFP@PPy@BSA nanoprobe at 25 $^{\circ}\text{C}$. After 4 h, 8 h, 12 h, and 16 h

incubation, the cells were washed with PBS (pH = 7.4) three times to remove the unabsorbed probe. The cells were scraped off by the cell scraper, and the suspension was centrifuged at 1500 rpm for 5 min. The precipitate was redispersed in PBS, and its ^{19}F NMR was measured on a Bruker Ascend WB 500 MHz spectrometer. Additionally, the PFP@PPy@BSA treated A549 cells were made biotransmission electron microscopy (Bio-TEM) specimens with standard procedures for observation.

***In vitro* photothermal therapeutic efficiency**

CCK8 assay: For photothermal therapy, the viability of cells with different treatments was evaluated by CCK8 assay. Briefly, A549 cells or MRC-5 cells (1×10^4) were seeded in 96-well plates and incubated with 200 μL of the serum-free medium containing PFP@PPy@BSA nanohybrid ($C_{\text{PFP}} = 6 \text{ mM}$) or PBS (pH 7.4, 10 mM) for 4 h, followed by 808 nm laser irradiation ($1 \text{ W}/\text{cm}^2$, 10 min) or not. Then the cell viability was measured by a microplate reader.

Confocal fluorescence imaging analysis: Briefly, A549 cells (1×10^5) were seeded into 6-well plates and incubated with the serum-free medium containing PFP@PPy@BSA nanohybrid ($C_{\text{PFP}} = 6 \text{ mM}$) or PBS (pH 7.4, 10 mM) for 4 h. After washing three times with PBS, the cells were exposed to 808 nm laser irradiation ($1 \text{ W}/\text{cm}^2$) for 10 min or not. After that, the cells were stained with Calcein AM/PI to probe living cells (green) and dead cells (red) and imaged by a confocal laser scanning fluorescence microscope (A1R/A1, Nikon, Japan).

Flow cytometry analysis: The death rate of cells with different treatments was determined by flow cytometry. Briefly, A549 cells (1×10^5) were seeded into 6-well plates and incubated with a serum-free medium containing PFP@PPy@BSA nanohybrid ($C_{\text{PFP}} = 6 \text{ mM}$) or PBS (pH 7.4, 10 mM) for 4 h. After incubation, the cells were washed three times in PBS and exposed to 808 nm laser irradiation for 10 min (1 W/cm^2) or not. Afterward, the cells were collected and stained by Annexin V-FITC/PI for 15 min and analyzed by flow cytometry (Beckman Coulter).

Animal and tumor model

Balb/c male nude mice (5-6 weeks of age, approximately 20 g) were purchased from Beijing Vital River Laboratory Animal Technology Co., Ltd. All experimental protocols in this study were approved by Animal Care and Use Committees at the Innovation Academy for Precision Measurement Science and Technology, the Chinese Academy of Sciences. To establish a subcutaneous A549 tumor model, Balb/c nude mice were subcutaneously inoculated on the leg with $100 \mu\text{L}$ 5×10^7 cells/mL of A549 cells suspended in PBS. After 4-5 weeks of breeding, the tumor-bearing mice could be used for *in vivo* experiments. To establish an orthotopic NSCLC model, Balb/c nude mice were anesthetized using tribromoethanol, and a total of 8×10^5 A549-Luciferase (A549-Luc) cells were directly injected into the left lung parenchyma of immunodeficient nude mice. Mice were monitored constantly until complete recovery from anesthesia.

Characterization of orthotopic NSCLC model mice

After 14 days of growth, the orthotopic NSCLC model mice were monitored by bioluminescence, CT, and MR imaging. The bioluminescence imaging was recorded on an IVIS spectrum system. The CT imaging was performed on a Micro-CT (Bruker Sky Scan 1176, Germany) with the following parameters: wave filter = A1-0.5 mm, X-ray voltage = 50 kV, Image resolution = 35 μ m. The *in vivo* ^{129}Xe MRI was performed on a 7.0 T animal MRI scanner (Bruker BioSpec 70/20 USR; Bruker, Ettlingen, Germany) using home-built double-tuned ($^1\text{H}/^{129}\text{Xe}$) birdcage coils with an inner diameter of 31 mm. Before MRI acquisition, the mice underwent one hyperpolarized ^{129}Xe pre-breath. The MRI acquisitions were triggered synchronously at the beginning of the second breath-hold with flash sequence (TR = 88.97 ms, TE = 3.52 ms, FOV = 3 cm \times 3 cm, 1.5 mm slice thickness with 10 slices, FA = 20°, matrix size = 64 \times 64, BW = 50 kHz).

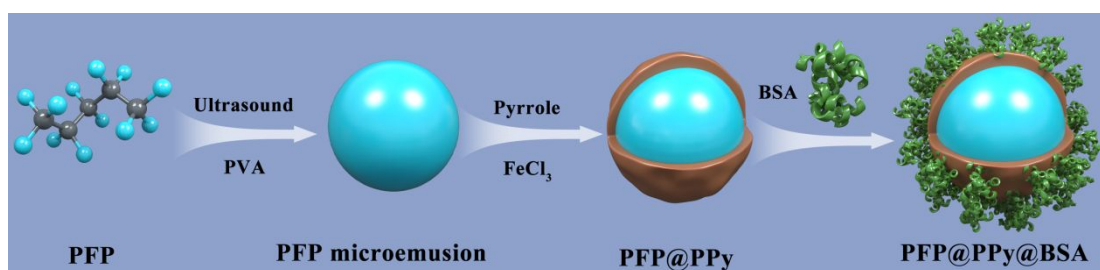
Hemolysis assay

The blood samples from healthy BALB/c mice were collected in EDTA-coated tubes, then red blood cells (RBCs) were isolated from serum by centrifugation at 2000 rpm for 10 min. The RBCs were further washed five times with 10 mL of sterile PBS. After the last wash, the RBCs were diluted to 20 mL with sterile PBS. Typically, for hemolysis measurement, 0.2 mL of the diluted RBCs suspension was added to 0.8 mL of PFP@PPy@BSA suspension in PBS with the PFP concentration of 1, 3, 6, 9, 12, and 18 mM. All the samples were incubated at 37 °C for 2 h and then centrifuged for 5 min at 5000 rpm. 200 μ L of supernatant of the sample tube was transferred to a

96-well chamber. The absorbance of the supernatant was measured at 541 nm using the ELISA plate reader (Spectra MAX 190, Molecular Devices). The corresponding hemolysis percentage values were calculated using the following formula: Hemolysis (%) = [(sample absorbance – negative control)/(positive control – negative control)] × 100%. RBCs incubated with deionized water and PBS were used as the positive and negative controls, respectively. The hemolysis measurement for each sample was repeated three times (Figure S17).

Statistical analysis

The data are expressed as the mean ± standard deviation. The *P*-value was analyzed using GraphPad Prism 9 (GraphPad Software, USA). *P* < 0.05 were considered statistically significant.



Scheme S1 Schematic illustration of the fabrication of PFP@PPy@BSA.

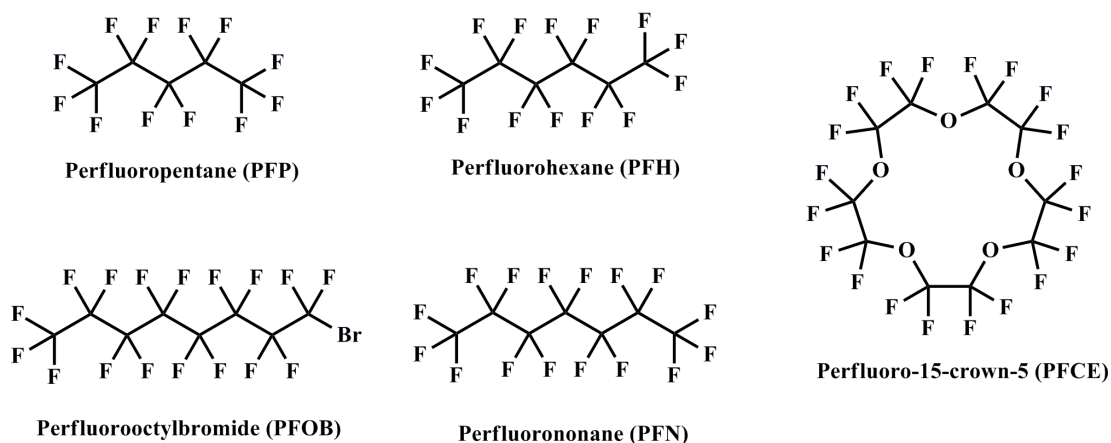


Fig S1. Structure of PFCs.

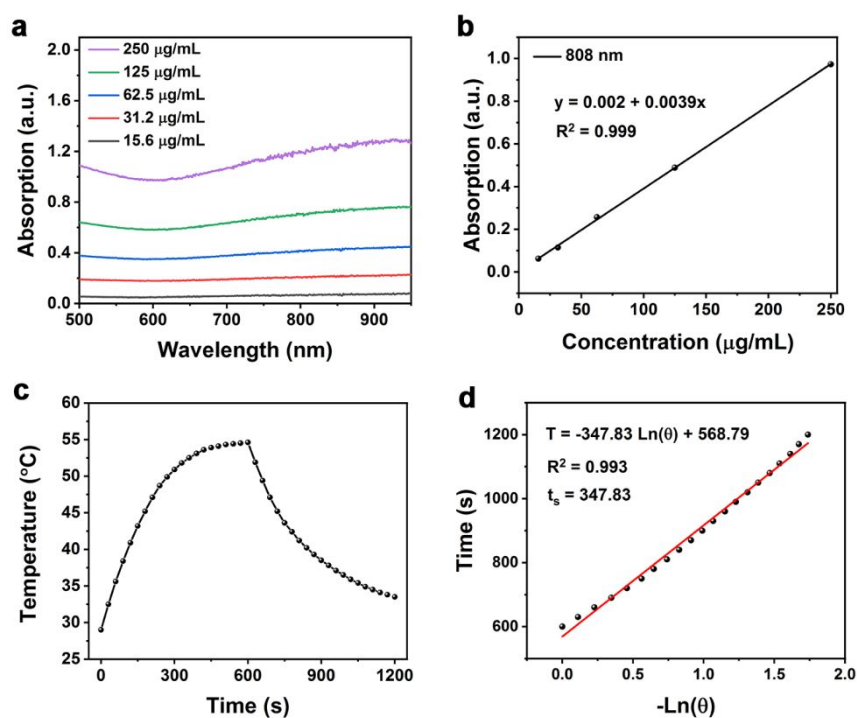


Figure S2 (a) UV-vis absorption spectra of PFP@PPy@BSA with different concentrations. (b) The standard curve of UV-vis absorption spectrum of PFP@PPy@BSA (808 nm). (c) Photothermal heating curve of PFP@PPy@BSA (125 $\mu\text{g/mL}$) under 808 nm laser irradiation (1 W/cm^2) for 10 min followed by cooling to room temperature. (d) Linear correlation of the cooling times versus negative natural logarithm of driving force temperatures.

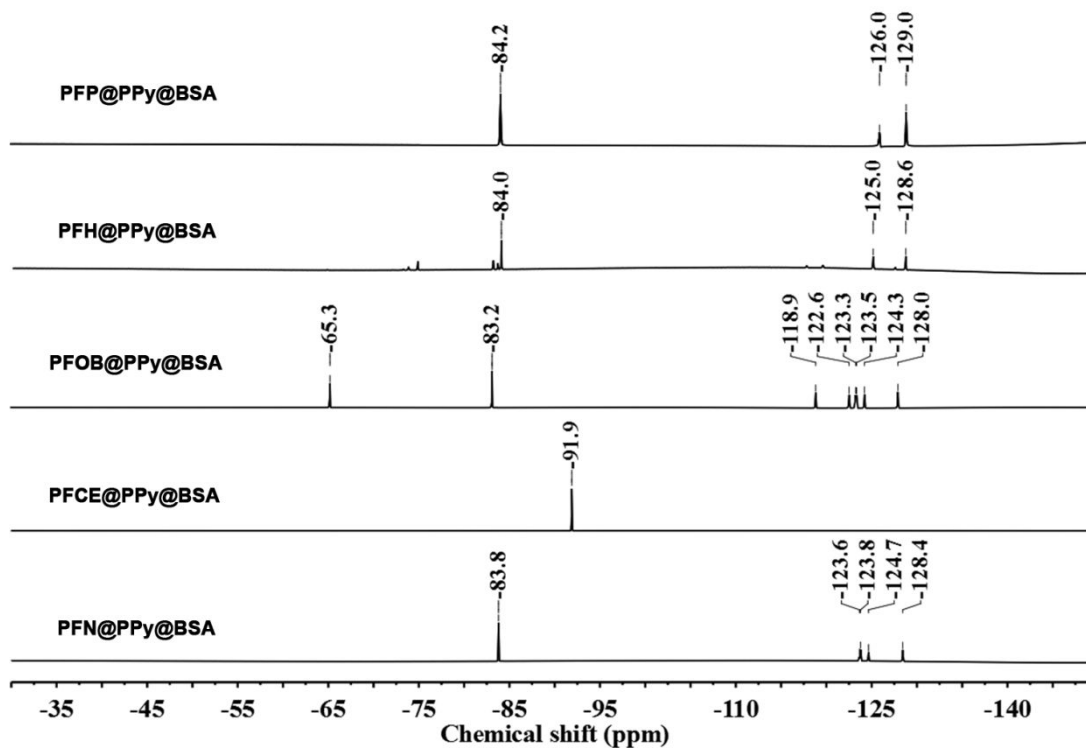


Figure S3 ^{19}F NMR of PFC@PPy@BSA.

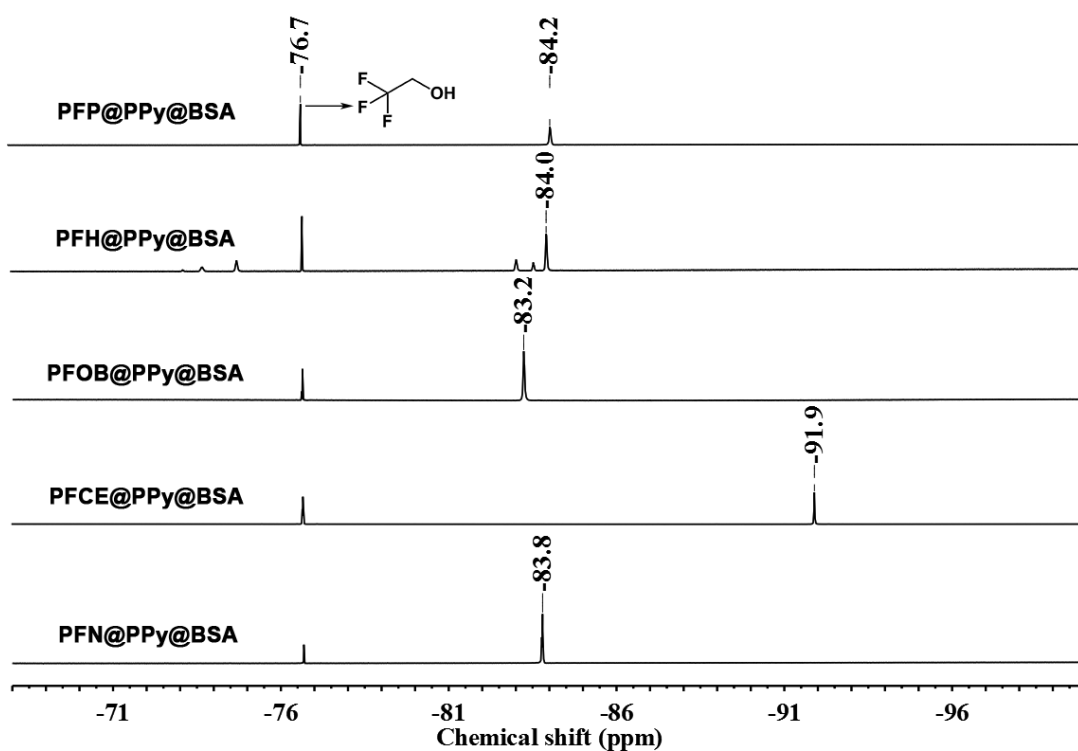


Figure S4 ^{19}F NMR of PFC@PPy@BSA (trifluoroethanol peak at -76.7 ppm).

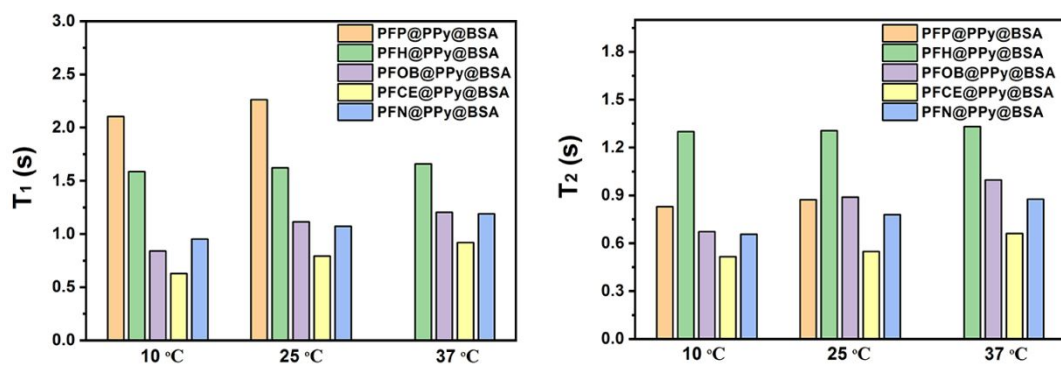


Figure S5 The relaxation times of PFC@PPy@BSA (PFC: $-\text{CF}_3$ or $-\text{CF}_2$) at different temperatures.

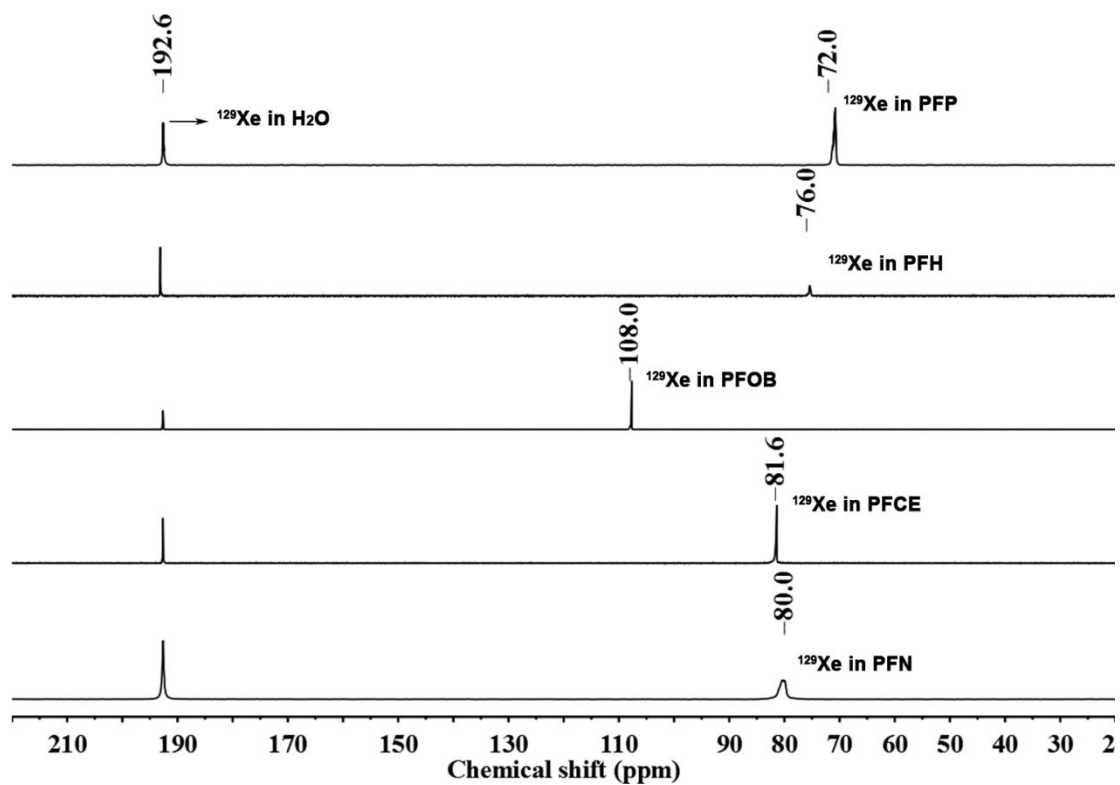


Figure S6 ^{129}Xe NMR of water and PFCs.

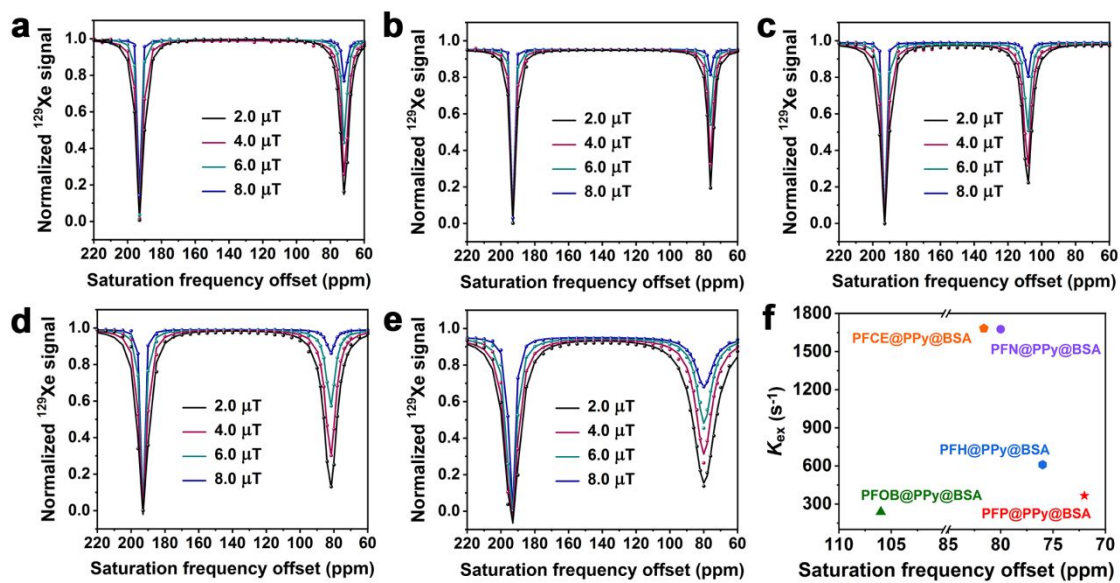


Figure S7 ^{129}Xe Hyper-CEST of PFC@PPy@BSA at different saturated pulse power.

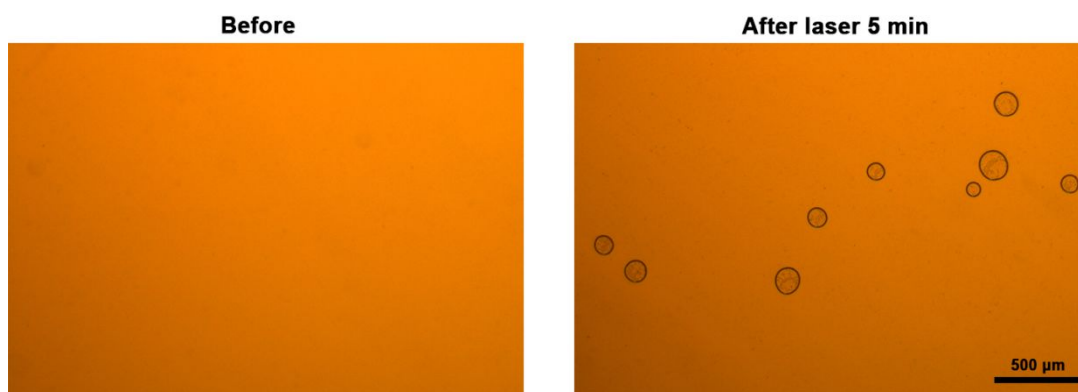


Figure S8 The generation of bubbles in PFP@PPy@BSA aqueous solution before and after laser irradiation for 5 min.

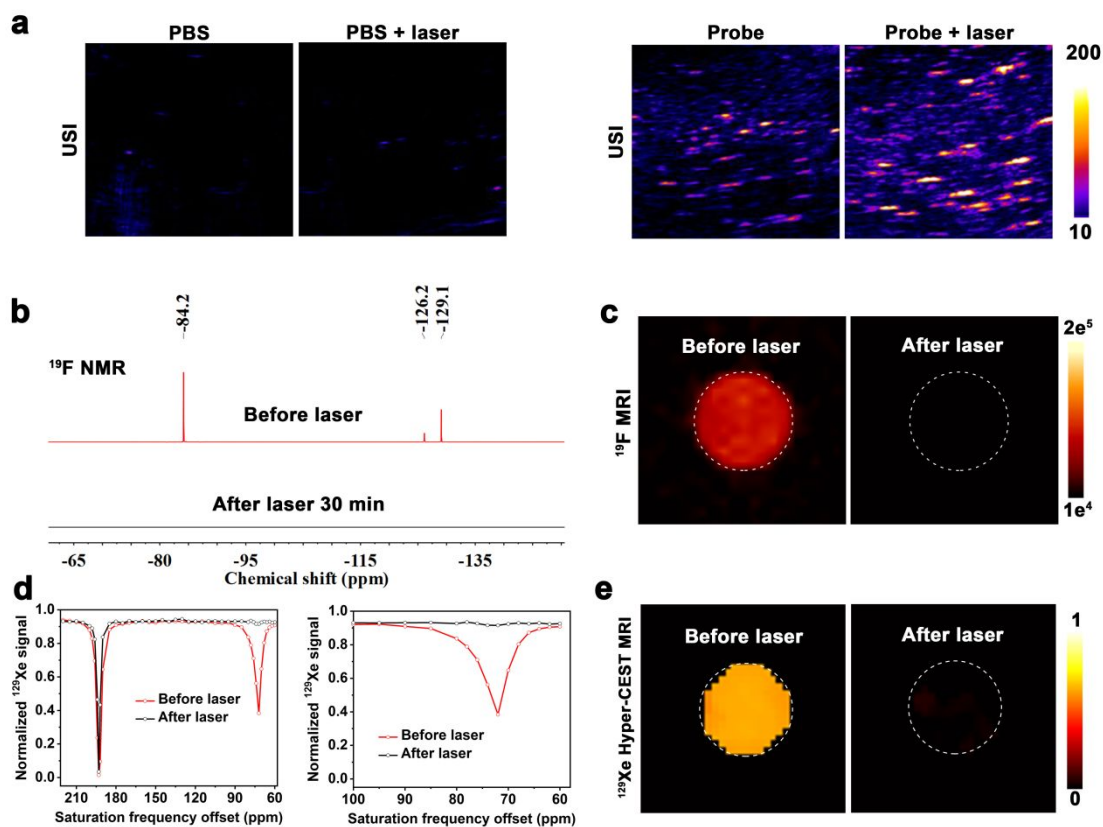


Figure S9 (a) US imaging of PBS and probe before and after laser irradiation. (b) ^{19}F NMR, (c) ^{19}F MRI, (d) ^{129}Xe Hyper-CEST and (e) ^{129}Xe Hyper-CEST MRI of PFP@PPy@BSA before and after laser irradiation.

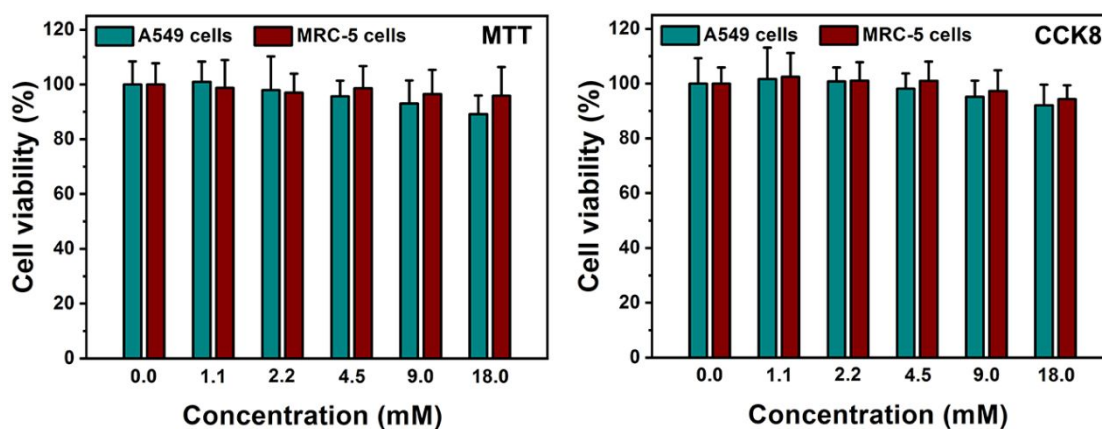


Figure S10 Cell cytotoxicity of PFP@PPy@BSA to A549 cells and MRC-5 cells incubated with 0–18 mM PFP for 24 h.

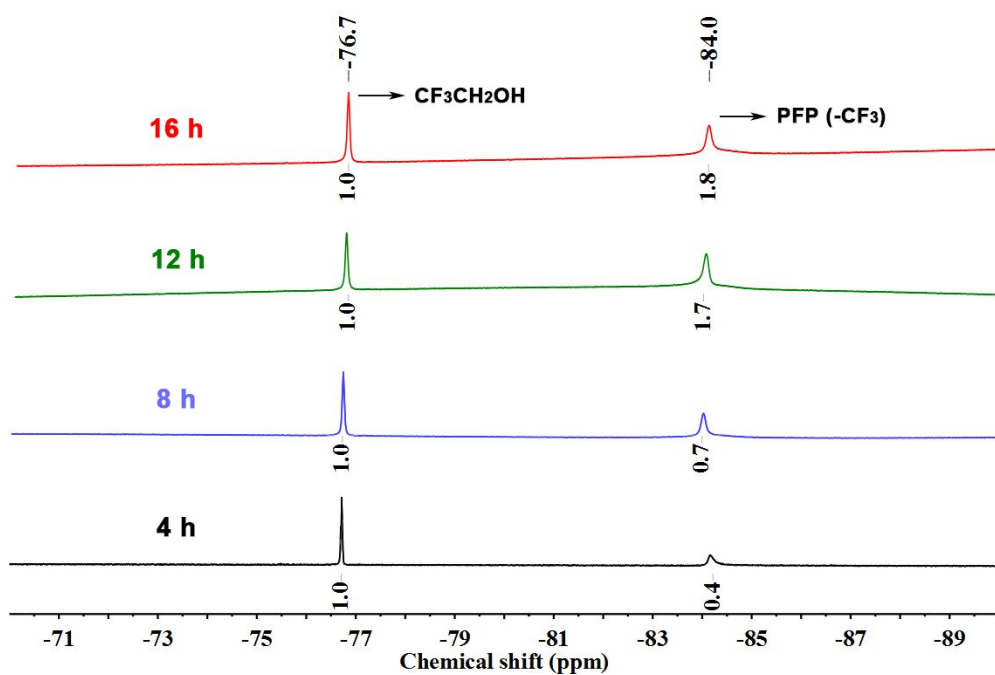


Figure S11 ¹⁹F NMR of A549 cells incubated with PFP@PPy@BSA for different times (trifluoroethanol peak at -76.7 ppm).

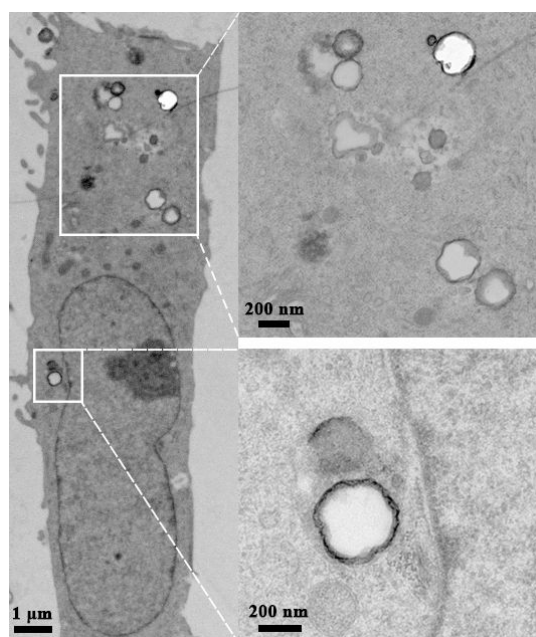


Figure S12 Representative bio-TEM images of A549 cells incubated with PFP@PPy@BSA.

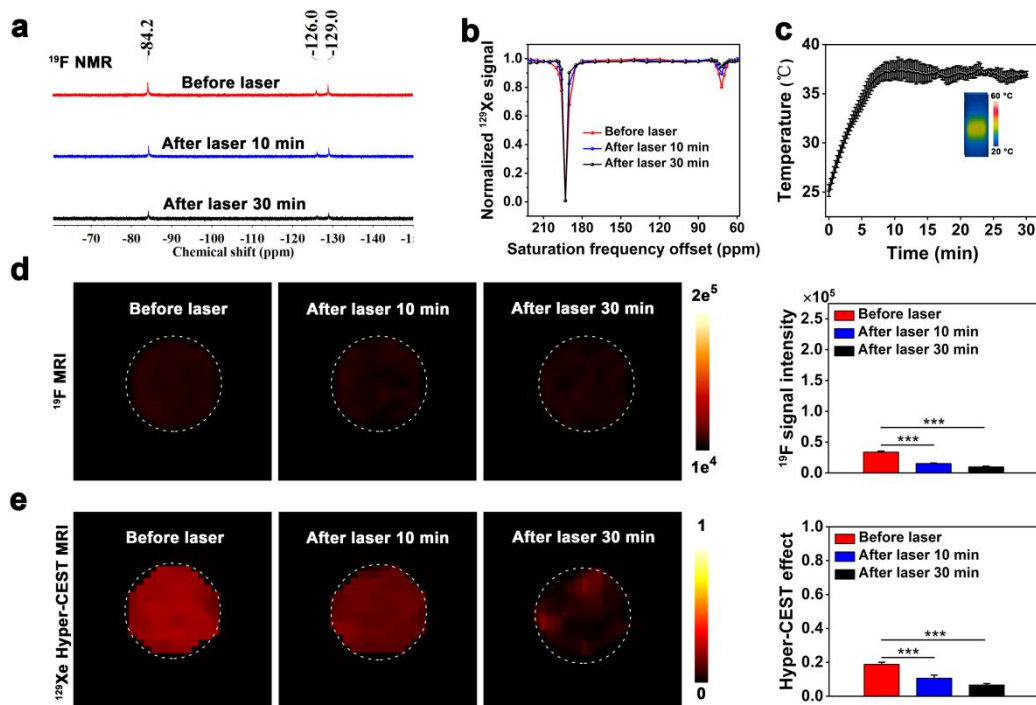


Figure S13 (a) ^{19}F NMR, and (b) ^{129}Xe Hyper-CEST spectra of MRC-5 cells treated with PFP@PPy@BSA. (c) Temperature changes of MRC-5 cells treated with PFP@PPy@BSA upon laser irradiation for 30 min. (d) ^{19}F MRI and the corresponding ^{19}F MRI signal intensity of MRC-5 cells treated with PFP@PPy@BSA before and after laser irradiation for 10 min and 30 min, respectively. (e) ^{129}Xe Hyper-CEST MRI and the corresponding Hyper-CEST effect of MRC-5 cells treated with PFP@PPy@BSA before and after laser irradiation for 10 min and 30 min, respectively. *** $P < 0.001$, $n = 3$, data represent mean \pm SD.

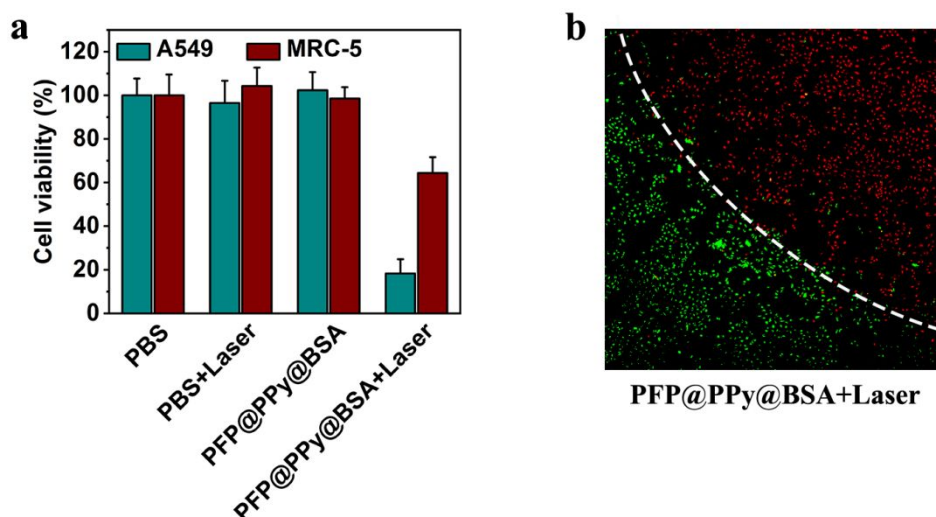


Figure S14 (a) Cell viability of A549 cells and MRC-5 cells treated with PBS, PBS + laser irradiation (808 nm, 1 W/cm², 10 min), PFP@PPy@BSA nanohybrid, and PFP@PPy@BSA nanohybrid + laser irradiation (808 nm, 1 W/cm², 10 min). (b) CLSM image of calcein-AM/PI labeling of A549 cells treated with PFP@PPy@BSA nanohybrid and laser irradiation (808 nm, 1 W/cm², 10 min).

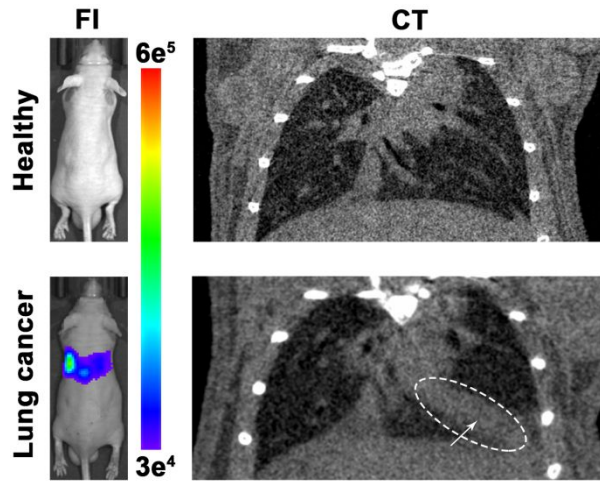


Figure 15 *In vivo* bioluminescence and CT imaging of healthy and orthotopic lung cancer mice.

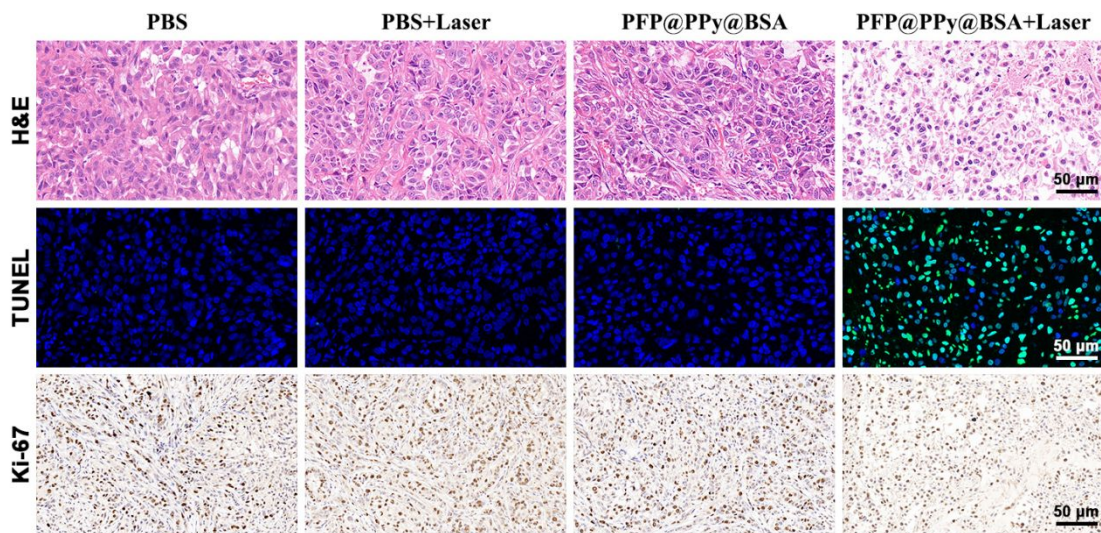


Figure S16 Tumor sections with H&E, TUNEL, and Ki-67 staining.

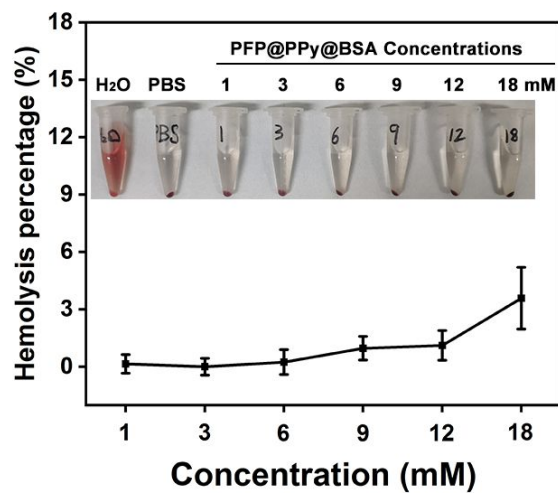


Figure S17 *In vitro* hemolysis percentage of PFP@PPy@BSA incubated with mice RBCs at 37 °C for 2 h at various concentrations ($C_{\text{PFP}} = 1, 3, 6, 9, 12,$ and 18 mM). RBCs incubated with PBS and deionized water were used as negative and positive controls, respectively.

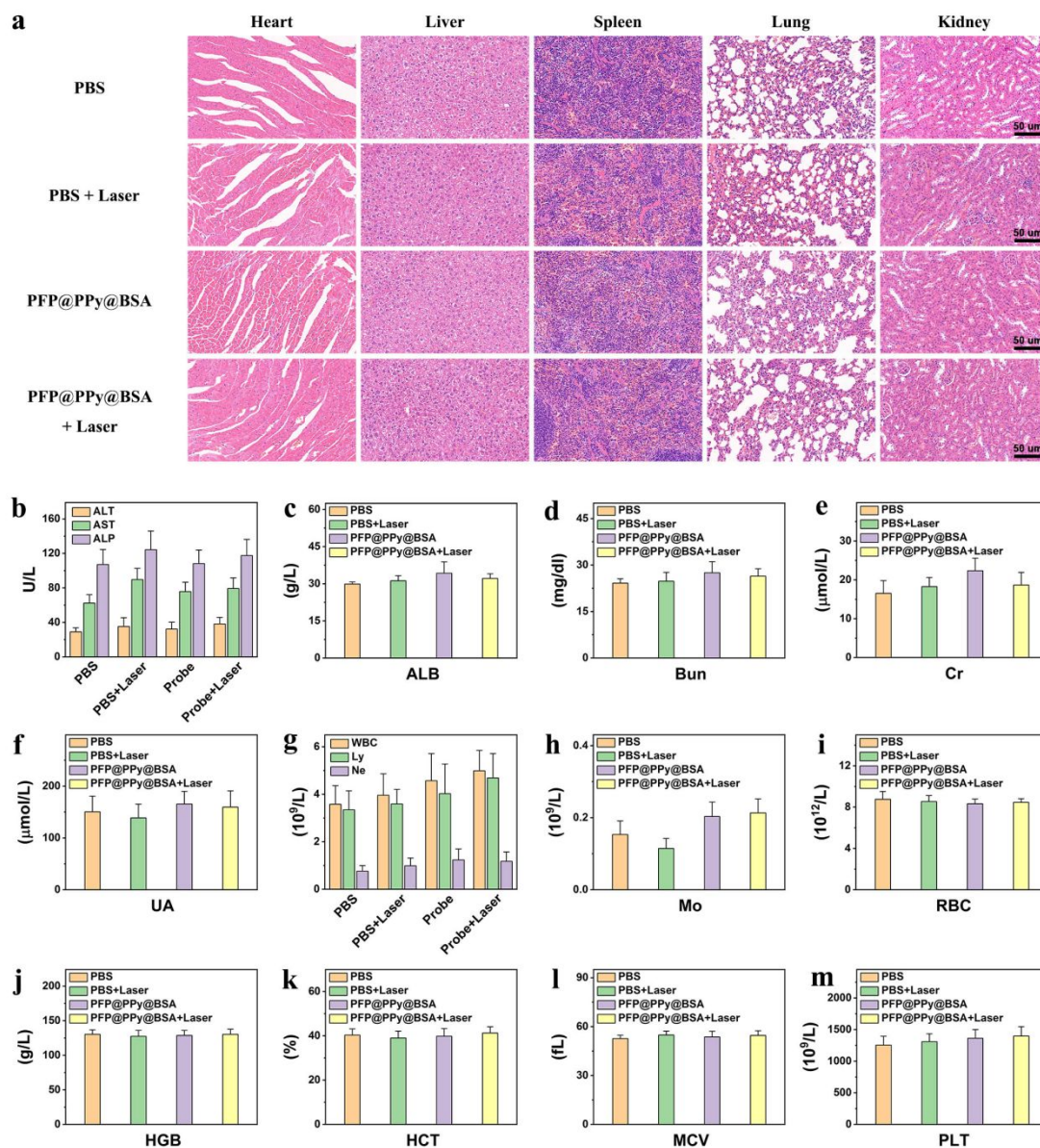


Figure S18 (a) Histological examination of heart, liver, spleen, lung, and kidney collected from different treatment groups. (b-m) blood indexes of ALT, AST, ALP, ALB, Bun, Cr, UA, WBC, Ly, NE, Mo, RBC, HGB, HCT, MCV, and PLT from various groups after 20 d treatment. Data are presented as mean \pm SD ($n = 3$).